

GROUND SUBSIDENCE CAUSED BY EARTHQUAKE TYPE EXCITATION

H. B. Poorooshasb¹ and A. Noorzad²

ABSTRACT: The extended CANAsand constitutive model, which incorporates the newly proposed concept of the "Compact State", is used in conjunction with the ID technique to evaluate the total subsidence of a sandy deposit. The ID technique is a simple numerical procedure developed recently. The results of the analysis clearly demonstrate the importance of the initial void ratio of the deposit, its permeability and the depth of the overburden on the magnitude of the subsidence of the layer.

INTRODUCTION

Ground subsidence of sandy layers in the event of a strong motion earthquake is a common occurrence. Such layers are found in many lowlands, deposited either naturally or by man (e.g. hydraulically filled reclaimed lands.)

The main objective of this paper is to present a simple method to evaluate the magnitude of the subsidence given certain information, the most important of which is the initial void ratio of the deposit, its depth and the depth of overburden.

The analysis is carried out with the aid of the CANAsand constitutive model which has recently been modified with the introduction of the concept of "Compact State" (Poorooshasb and Noorzad 1996; Noorzad 1998), and a simple numerical technique developed jointly with researchers at Institute of Lowland Technology, Saga University and called the ID technique (Poorooshasb et al 1996).

This presentation is written in the following sequence. First the concept of "compact state" and its relation to the "critical state" is discussed and the CANAsand constitutive model formulated in the light of these two concepts. Next the analysis of the sand layer is carried out. Presenting some results of the analysis concludes the paper.

CANAsand MODEL

The Compact State

The state of an isotropic soil element may be represented by the set of three stress related quantities (p, q, θ) and the void ratio of the element e . The quantities p, q and θ are related to the effective stress tensor σ_{ij} by the equations as follows:

$$\left. \begin{aligned} p &= I_1 / \sqrt{3}; & I_1 &= \sigma_{ii} \\ q &= J_2 / \sqrt{2}; & J_2 &= (s_{ij}s_{ij})^{1/2} \\ \theta &= \frac{1}{3} \sin^{-1} \left(-\frac{3\sqrt{3}J_3}{2q^3} \right); & J_3 &= (s_{ij}s_{jk}s_{ki})^{1/3} \end{aligned} \right\} \quad (1)$$

1 Professor, Department of Building, Civil and Environmental Engineering Concordia University, Montreal, CANADA.

2 Director General, Water Supply, Ministry of Energy, Tehran, IRAN.

Note: Discussion on this paper is open until June 1, 2000.

where $s_{ij} = \sigma_{ij} - \sigma_{kk}\delta_{ij}/3$ is the stress deviation tensor. The total strain rate is given by the equation as follows:

$$\dot{\bar{\epsilon}} = \dot{\epsilon}_{ij}^e + \dot{\epsilon}_{ij}^p \quad (2)$$

where $\dot{\epsilon}_{ij}^e$ is the elastic and $\dot{\epsilon}_{ij}^p$ the plastic components of the strain rate tensor respectively. Plastic distortion rate of the element is

$$\dot{\bar{\epsilon}} = (\dot{d}_{ij}^p \dot{d}_{ij}^p)^{1/2}; \quad \dot{d}_{ij}^p = \dot{\epsilon}_{ij}^p - \dot{\epsilon}_{kk}^p \delta_{ij} / 3 \quad (3)$$

Thus the total plastic distortion is given by

$$\bar{\epsilon} = \int \dot{\bar{\epsilon}} dt \quad (4)$$

where t is some convenient time scale. At the Critical State an element experiences unbounded distortion. Thus

$$\bar{\epsilon}(p, q, \theta, e) \rightarrow \infty \quad (5)$$

where all the quantities within the bracket are at their critical values. In contrast at Compact State the element does not experience any plastic distortion (it behaves as a purely elastic material) and one has

$$\dot{\bar{\epsilon}}(p, q, \theta, e) = 0 \quad (6)$$

where all the quantities within the bracket are at the values related to the compact state.

A physical interpretation of the Critical as well as the Compact States is in order. The Critical State is reached under an essentially monotonically increasing loading program and represents a very "loose" state of the sample; i.e. the void ratio at the Critical State is very

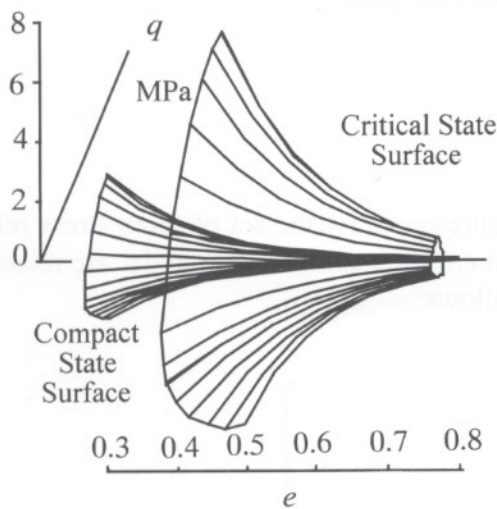


Fig. 1 The isometric view of the Critical and the Compact State Surfaces, $\phi_{crit} = 30^\circ$, $\phi_{comp} = 45^\circ$

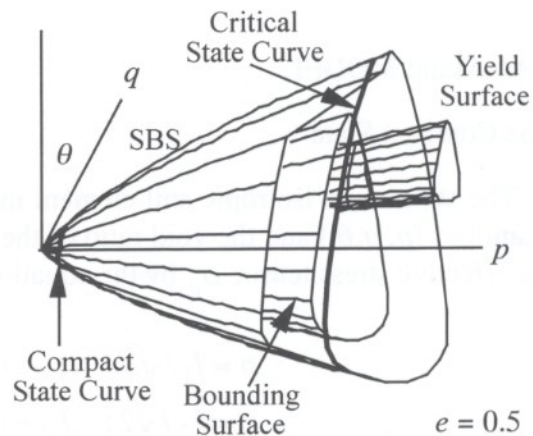


Fig. 2 Trace of the Critical and the Compact State Surfaces on the State Boundary Surface

high. In contrast the void ratio at the compact state is at its lowest possible value and one has to use a cyclic loading program (say by shaking) to achieve it.

The set of four quantities p, q, θ, e , when at their critical values, lie on a surface called the Critical State Surface in a four dimensional space of (p, q, θ, e) which, of course, can not be shown on a two dimensional sheet of paper. However if use is made of a celebrated equation by Casagrande who suggests that a simple relation exist between the Critical e and Critical p in the form $e = e_0 - \lambda \ln(p/p_0)$, then the number of independent variables can be reduced to three. Thus an isometric representation of the Critical State Surface is possible, see Fig. 1. Note that the two quantities e_0 and p_0 are two conveniently chosen datum constants.

Shown in Fig. 1 is also an isometric representation of the Compact State Surface. To obtain this surface a fundamental law of similarity has been evoked, which appears to have stood the test of time (Roscoe and Poorooshasb 1963).

Figure 2 shows the State Boundary Surface (SBS), the Bounding Surface (Dafalias and Popov 1975) and the Yield Surfaces for a constant value of void ratio $e = 0.5$. The Critical and the Compact States trace two distinct curves on the SBS. A sand element may, theoretically, experience all states within the SBS. If the state point lies to the left of the vertical plane containing the Compact State Curve and the origin then its behavior would be purely elastic; otherwise it may experience both elastic and plastic distortions.

Let parameters η and e' be defined by

$$\eta = \frac{q}{pg(\theta)}; \quad e' = e_0 - \lambda \ln \frac{p}{p_0} - e \quad (7)$$

where $g(\theta)$ is a specific function defining the curvature of the State Boundary Surface in the so called π plane. If this surface were a *cone* with its apex on the origin of the stress space and the axis along the space diagonal then the function $g(\theta) = 1$. For convince $g(0)$ is set equal to 1.

The function φ is defined by

$$\varphi = \mu + e'\delta - \eta \quad (8)$$

where μ and δ are two material constants. Parameter μ defines the slope of the Critical State Line in the p, q space when $\theta = 0$ (and hence $g(\theta) = 1$) and δ is the interlocking angle.

In the CANASand Model it is postulated that at the State Boundary this function is zero; i.e.

$$\varphi|_{SBS} = 0 \quad (9)$$

Formulation of the Constitutive Law in terms of State Parameters

The existence of a plastic potential in the form

$$\psi = p\bar{\psi}(\eta, e') \quad (10)$$

is assumed. Thus the plastic strain rate is given by

$$\dot{\epsilon}_{ij}^p = \dot{\gamma} \frac{\partial \psi}{\partial \sigma_{ij}} \quad (11)$$

where $\dot{\gamma}$ is a scalar to be determined in order to establish the constitutive equation. From the last equation, the plastic distortion rate is

$$\dot{\bar{\epsilon}} = \dot{\gamma} \left[\text{dev} \left(\frac{\partial \psi}{\partial \sigma_{ij}} \right) \text{dev} \left(\frac{\partial \psi}{\partial \sigma_{ij}} \right) \right]^{1/2} \quad (12)$$

where $\text{dev}(\partial \psi / \partial \sigma_{ij}) = \partial \psi / \partial \sigma_{ij} - (\partial \psi / \partial \sigma_{kk}) \delta_{ij} / 3$. On the other hand the total plastic distortion has been found, experimentally, to have a simple (hyperbolic) relationship to the state variables in the form as follows:

$$\bar{\epsilon} = a \eta / \varphi \quad (13)$$

where φ is defined by Eq. (1) and $a = a(e')$. Let

$$e_{\kappa} = e_0 - \lambda \ln(p / p_0) - e_{comp} = e_{crit} - e_{comp} \quad (14)$$

where e_{comp} is the void ratio of the element at the compact state. Then to ensure that at this state no plastic deformation takes place the condition $a(e_{\kappa}) = 0$ must hold. From Eq. (13) the rate of plastic distortion is obtained as follows:

$$\dot{\bar{\epsilon}} = \frac{1}{\varphi^2} [a(\varphi + \eta)\dot{\eta} + \eta(a'\varphi - a\delta)\dot{e}'] \quad (15)$$

where $a' = da / de'$ and $\dot{e}' = -\lambda \dot{p} / p - \dot{e}$. Thus

$$\dot{\bar{\epsilon}} = (f_1 + f_2) / \varphi^2 \quad (16)$$

where

$$f_1 = a(\varphi + \eta)\dot{\eta} + a\eta\lambda\delta\dot{p} / p \quad (17)$$

and

$$f_2 = \eta(a\delta + a'\varphi) \quad (18)$$

But the rate of volume change \dot{v} is given by

$$\dot{v} = \dot{e} / (1 + e) = \dot{\epsilon}_{ii}^e + \dot{\epsilon}_{ii}^p = \dot{p} / K + \dot{\gamma} \partial \psi / \partial \sigma_{ii} \quad (19)$$

where K is the elastic bulk modulus, leading to $\dot{e} = (1 + e)\dot{p} / K + \dot{\gamma}(1 + e)\partial \psi / \partial \sigma_{ii}$. Inserting this value in Eq. (16) and combining the results with Eq. (12) results in the value of $\dot{\gamma}$, viz.

$$\dot{\gamma} = \frac{f_1 + f_2 \cdot (1 + e) \dot{p} / K}{-(1 + e) f_2 \frac{\partial \psi}{\partial \sigma_{ii}} + \varphi^2 \left(\text{dev} \frac{\partial \psi}{\partial \sigma_{kl}} \text{dev} \frac{\partial \psi}{\partial \sigma_{kl}} \right)^{1/2}} \quad (20)$$

Thus the constitutive relation is established, i.e. the total strain rate can be evaluated if the stress rate is specified. In most numerical applications this form is of little use. To obtain the

stress rate, in terms of the strain rate, denote the numerator of the Eq. (20) by f_3 and note that $\dot{\eta} = (\partial\eta / \partial\sigma_{ij})\dot{\sigma}_{ij}$. Then after some simple manipulations one may write Eq. (20) as follows:

$$\dot{\gamma} = \frac{\chi_{ij}}{f_3} \dot{\sigma}_{ij} \quad (21)$$

where

$$\chi_{ij} = a(\varphi + \eta) \frac{\partial\eta}{\partial\sigma_{ij}} + \frac{1}{\sqrt{3}} \left[\frac{a\eta\lambda\delta}{p} + \frac{(1+e)f_2}{K} \right] \delta_{ij} \quad (22)$$

Thus the constitutive equation may be stated as follows:

$$\dot{\sigma}_{ij} = G_{ijkl}^{ep} \dot{\epsilon}_{kl} \quad (23)$$

where $G_{ijkl}^{ep} = [C_{ijkl} + (\chi_{ij} / f_3)(\partial\psi / \partial\sigma_{kl})]^{-1}$ are the elastic-plastic moduli and C_{ijkl} are the elastic moduli.

ANALYSIS

Statement of the Problem

A layer of sand of total height H is subjected to a random horizontal excitation at its base (say the bedrock, see Fig. 3). The void ratio of the sand is assumed to vary slightly with depth (due to consolidation by self weight and the load imposed by the surcharge) otherwise the layer is assumed to be homogeneous. The surcharge is assumed to be either free draining or otherwise totally impervious. The ground water is located at the grade level, Fig. 3.

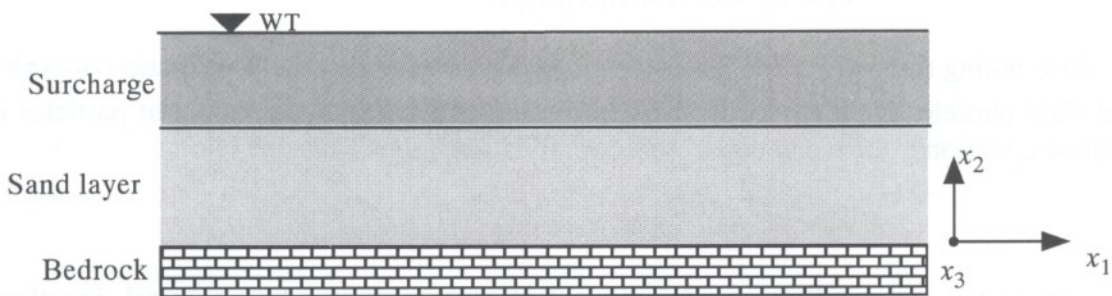


Fig. 3 Sand layer over bedrock. Note the coordinate system used

The random excitation at the base is given by the following equation

$$\dot{v}_1(x_1, 0, x_3) = \sum_{n=1}^{n \max} \langle t_n \rangle \exp(-\alpha_n t_n) \sin(\omega_n t_n); \quad \dot{v}_2(x_1, 0, x_3) = \dot{v}_3(x_1, 0, x_3) = 0 \quad (24)$$

where $t_n = t - T_n$, and the symbol $\langle \rangle$ denotes the singularity brackets. Quantities T_n , α_n and ω_n are random values and $n \max$ is the maximum number of terms used in the finite series.

The particular form of the excitation used in this paper for all the cases cited is shown in Fig. 4.

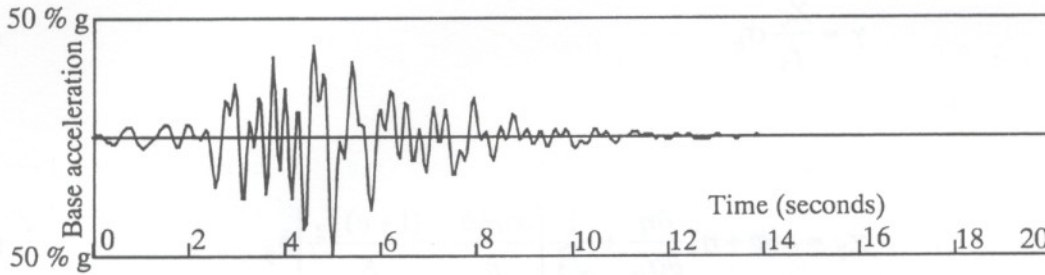


Fig. 4 Horizontal component of base acceleration used in this study

The set of equations describing the interaction between the soil and water particles in a dynamic loading process is

$$\left. \begin{aligned} \frac{\partial \sigma'_{ij}}{\partial x_j} + n^s \frac{\partial u}{\partial x_i} + D_{ij}(v_j^s - v_j^f) + \rho^s n^s \frac{\partial v_i^s}{\partial t} &= 0 \\ n^f \frac{\partial u}{\partial x_i} - D_{ij}(v_j^s - v_j^f) + \rho^f n^f \frac{\partial v_i^f}{\partial t} &= 0 \end{aligned} \right\} \quad (25)$$

where the small strain theory is used. In Eq. (25) σ'_{ij} is the effective stress felt by the soil particles, u is the pore water pressure, n^s and n^f are the solid and fluid porosity respectively D_{ij} is the drag coefficient ρ^s and ρ^f are the density, and v_i^s and v_i^f the velocity vectors, of the solid and the water phases respectively.

Since the excitation is along the x_2 axis only, Eq. (9), one can show, using the argument of similarity that

$$v_3^s = v_3^f = 0 \quad \text{for all } x_1, x_2, x_3 \quad (26)$$

Also noting that $\dot{v}_2(x_1, 0, x_3) = 0$ then it may be argued that the acceleration of both solid and fluid particles are confined to the x_1 direction. That is, the movement of particles in the vertical direction is slow and due to soil consolidation only. Thus one has

$$\dot{v}_2^s = \dot{v}_2^f = 0 \quad \text{for all } x_1, x_2, x_3 \quad (27)$$

In view of the last conditions and for $I = 2$ (i.e. movement in the vertical direction) the second equation of the set of Eq. (25) reduces to

$$\frac{\partial u}{\partial x_2} - \frac{D_{21}}{n^f}(v_1^s - v_1^f) - \frac{D_{22}}{n^f}(v_2^s - v_2^f) = 0 \quad (28)$$

And since $D_{21} = 0$ in view of the assumption regarding soil isotropy then the last equation reduces to

$$\frac{\partial u}{\partial x_2} - \frac{D_{22}}{n^f}(v_2^s - v_2^f) = 0 \quad (29)$$

which merely indicates a process of consolidation in the vertical direction. Finally if the two equations of the set (25), are added one obtains, after some simple rearrangement of terms, the dynamic equation of motion, viz.

$$\frac{\partial \tau}{\partial z} = \frac{\gamma}{g} \frac{\partial v}{\partial t} \quad (30)$$

where $\tau = (-\sigma_{21})$ is the shear stress on a horizontal plane, v is the velocity of a solid particle, g is the gravity and $\gamma = g(\rho^s n^s + \rho^f n^f)$ is the total unit weight of the soil element. The variable $z (= x_2)$ and t are space and time coordinates respectively.

The numerical evaluation of Eq. (29) is relatively simple and a finite difference scheme was employed. For evaluation of Eq. (30) the ID technique was used.

The ID technique is a simple numerical procedure developed jointly by the researchers at Concordia University, Canada and the Institute of Lowland Technology, Saga University, Japan to analyze a certain type of plane strain and axisymmetric problems, see Poorooshasb et al (1996). It is called the ID technique because it evaluates an Integro-Differential equation.

Differentiation of Eq. (30) with respect to time yields the equation as follows:

$$\frac{\partial \dot{\tau}}{\partial z} = \frac{\gamma}{g} \frac{\partial^2 v}{\partial t^2} \quad (31)$$

noting that $\dot{\gamma}$ is small and may be neglected. Integrating the two sides of the last equation with respect to z results in the equation as follows:

$$\dot{\tau} = \frac{1}{g} \int_0^z \gamma(\xi) \frac{\partial^2 v(\xi, t)}{\partial t^2} d\xi \quad (32)$$

But $\dot{\tau} = G^{ep} (\partial v / \partial z)$ where G^{ep} is the elastic-plastic shear modulus in simple shear. Combining the last two equations results in the Integro-Differential form of the governing equation, viz.

$$\frac{\partial v}{\partial z} = \alpha(z) \int_0^z \gamma(\xi) \frac{\partial^2 v(\xi, t)}{\partial t^2} d\xi \quad (33)$$

where $\alpha(z) = [gG^{ep}(z)]^{-1}$.

Numerical Evaluation of Equation (33)

The numerical evaluation of Eq. (33) is very simple. Consider node (i, j) in the (z, t) space, Fig. 5 (a). Then Eq. (33) can be broken into its finite difference form as follows:

$$v_{i+1,t} - v_{i,t} = \beta(i) \left[\frac{1}{2} \gamma(1)(v_{1,t+} - 2v_{1,t} + v_{1,t-}) + \sum_{j=2}^i \gamma(j)(v_{j,t+} - 2v_{j,t} + v_{j,t-}) \right] \quad (34)$$

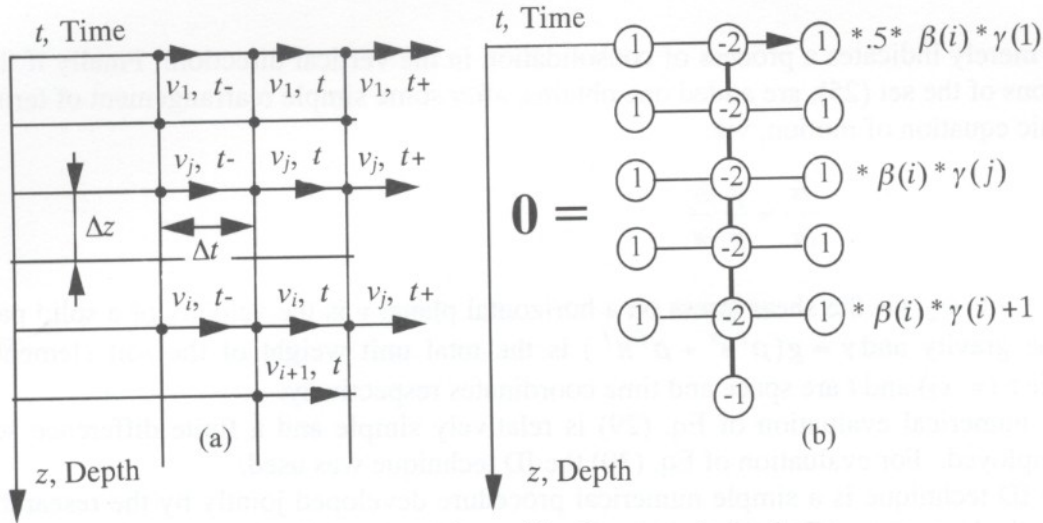


Fig. 5 (a) The network used in the numerical scheme
(b) Graphical representation of the operations

Assuming that the values of v for all nodal points just before and at the present time t (i.e. $v_{j,t-}$ and $v_{j,t}$) are known Eq. (34), together with the boundary value at the bedrock at the present time provide enough equations to predict the velocity of the soil particle at the time $t+$. Note that in Eq. (34); $\beta(i) = \alpha(i)(\Delta z^2 / \Delta t^2)$.

The graphical representation of the above operation is shown in Fig. 5 (b).

Results of the Numerical Analysis

Having broken Eq. (34) into a set of linear algebraic equations the first task is, of course, to ensure the stability and uniqueness of the solution. Since the constitutive equation is non-linear some iterative process is required. In this paper the process known as the one step Newton-Raphson correction is used and the results appear to be satisfactory provided a sufficiently small time step ($\Delta t = 0.0025$) is used.

Figure 6 is the key figure for the results presented in this paper. It shows the contours of the pore water pressure at the various time stages during the action of the strong ground motion. Note that when curve titled "p.w.p at $t > 0$ " touches the "total vertical stress for all t " then liquefaction of the layer is imminent (i.e. the effective vertical stress is zero).

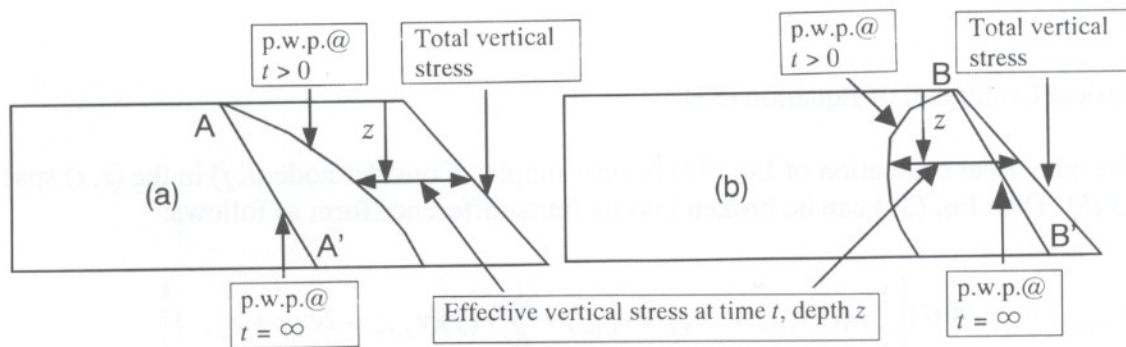


Fig. 6 Key figures: (a) Surcharge free draining, (b) Surcharge impervious

If the surcharge is free draining then the pore water pressure at time infinity will tend to the line AA' indicated in Fig. 6 (a) which represents the hydrostatic water pressure. For impervious surcharge the distribution of the pore water pressure approaches the line shown in Fig. 6 (b) as BB' which is the hydrostatic plus the pressure due to the weight of the surcharge.

In all tests reported here the depth of the sand layer was kept constant and equal to 3 meters. As a first series of tests the performance of the system was examined using a range of values for the coefficient of permeability, k , ranging from .01 to 10 cm/sec, see Fig. 7. In all these tests the soil was assumed to be extremely loose ($e = 0.8$) and the surcharge was taken equal to zero. As expected very little subsidence took place during the period of strong motion when the permeability is low ($k = 0.01$ cm/sec). That is, most of the subsidence would take place after the shaking event. On the other hand, the extremely permeable sand layer, $k = 10$ cm/sec, subsides during the shaking period. Since highly permeable sands cause a particular type of situation the coefficient of permeability in all other tests reported here is taken to be equal to 5 cm/sec.

To investigate the effect of overburden pressure (surcharge) on the performance of the system a series of tests were conducted with surcharge values ranging from 2 meters to 10 meters of free draining soil with a total unit weight of 19 kN/m^3 . The results are shown in Fig. 8. Note that the subsidence under the heavy surcharge of 10 m, (20 cm) is somewhat smaller than that under the light surcharge of 2 m, (29 cm) and less than two thirds of the case with no surcharge, (34 cm). Note that the curve for this case is not shown in this Fig. 9. This finding is of some interest. With an increase in the overburden pressure the sand consolidates and as a result its representation in the $e-p$ space gets closer to the so called Casagrande's critical void ratio line. Thus the material is considered to be more prone to liquefaction and an increasing value of subsidence. Exactly the opposite is observed. But the reason is quite simple: Although the soils condition are closer to its critical yet the increase in the vertical stress associated with an increase in the magnitude of surcharge causes a much stiffer response from the soil element resulting in a smaller magnitude of ground settlement.

Surcharges used in the above tests were assumed to be all free draining. In the next series of tests they were assumed to be completely impervious. The results of these tests showed that the presence of impervious surcharge made very little difference to the variation of form or the magnitude of subsidence recorded. It is emphasized that here the term subsidence means the settlement of the sand layer surface; the ground surface will not subside at all! It will simply float on a layer of water. Formation of sand volcanoes, eruption of sand around footings and appearance of large cracks in clay layers supported by a layer of sand are considered to be the results of such a phenomenon, Fig. 10.

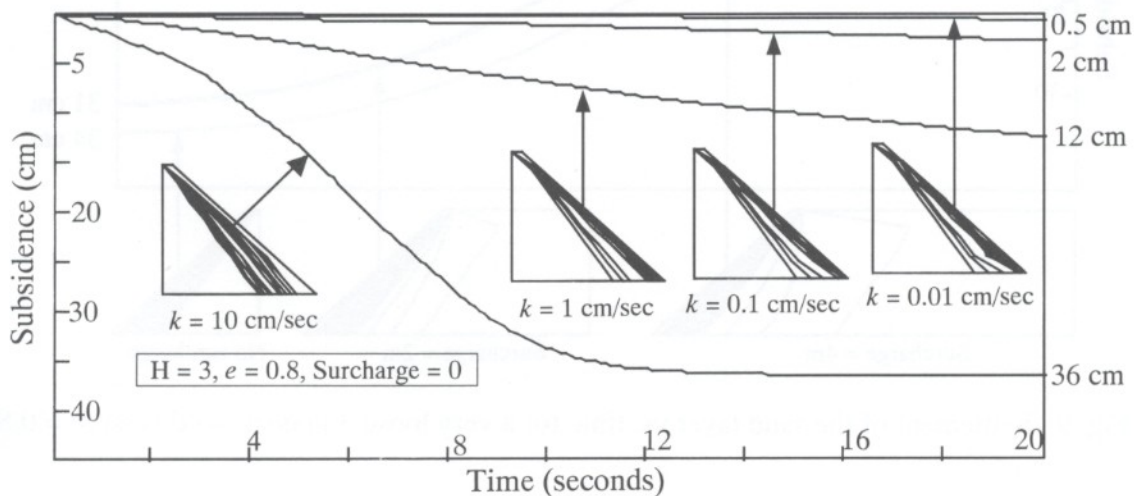


Fig. 7 Subsidence/time curves for various coefficients of permeability

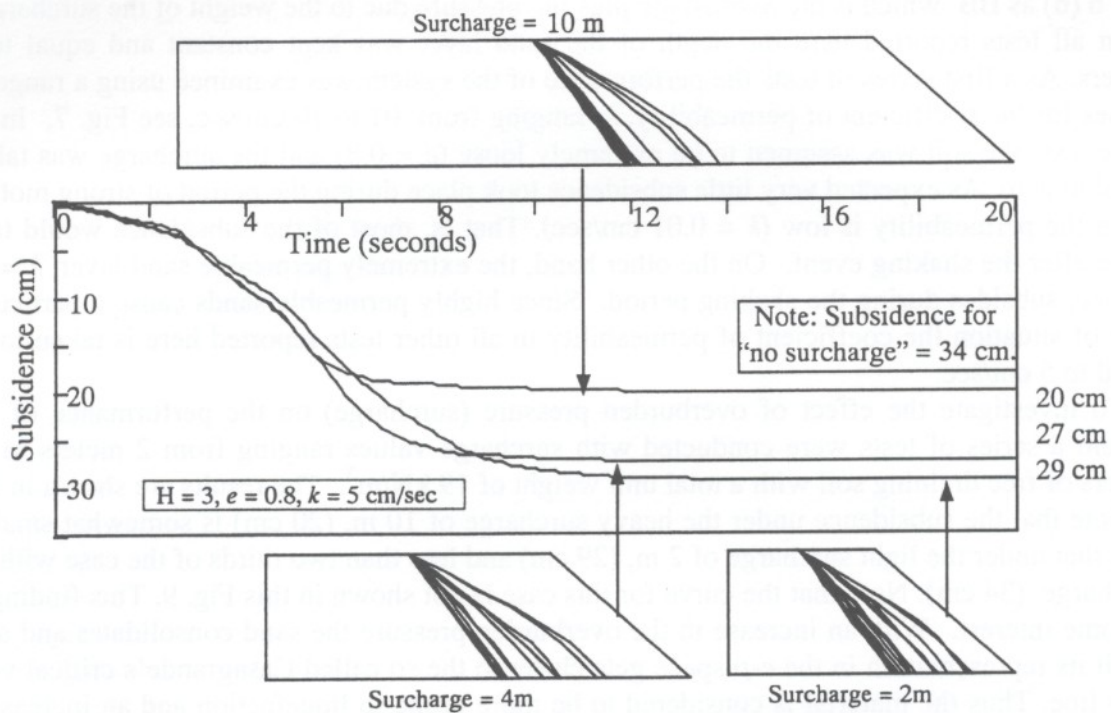


Fig. 8 Ground subsidence/time curves for various free-draining surcharge values

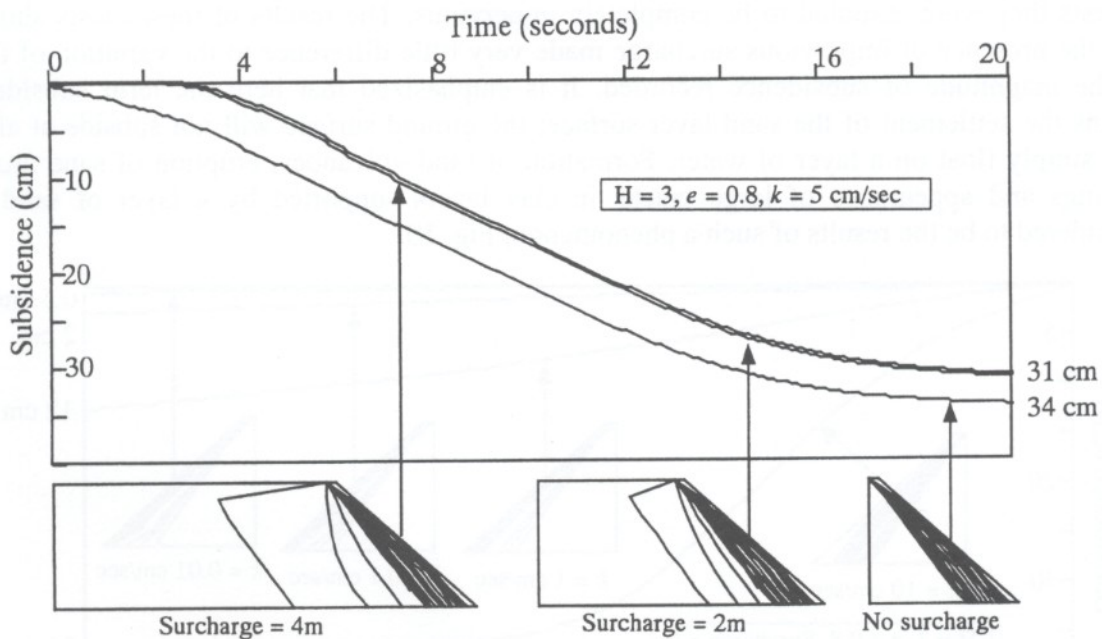


Fig. 9 Settlement of the sand layer vs. time for a very loose 3 m deep sand layer, $e = 0.80$

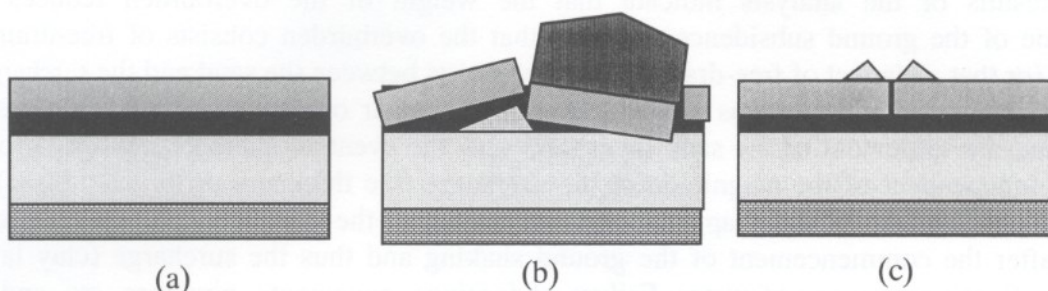


Fig. 10 (a) Two forms of instability caused by clay layer (surcharge) floating on a film of water
 (b) Overturning of structure
 (c) Sand volcanoes

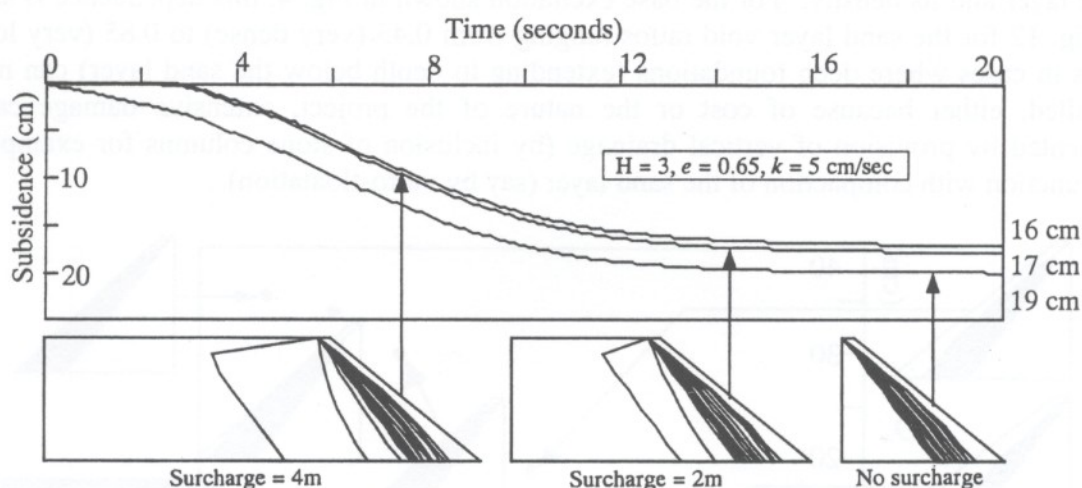


Fig. 11 Settlement of the sand layer vs. time for a medium dense 3 m deep sand layer, $e = 0.65$

The fact that settlement/time curves show little sensitivity to the magnitude of the surcharge can easily be explained. Shortly after the commencement of ground shaking the layer of water appears on the top of the sand layer effectively separating the surcharge from the supporting sand layer. Hence onwards the sand layer behaves as if it is not carrying any surcharge at all: It is the water that bears the weight of the overburden pressure and not the sand layer.

The void ratio for all the above cases was taken to be equal to 0.8 indicating a very loose sand sample. Three more tests were performed with a sand layer having an average void ratio of 0.65. The results shown in Fig. 11 confirm the previous observation regarding the insensitivity of sand layer settlement to the magnitude of the impervious surcharge.

CONCLUDING REMARKS

The extended CANAsand model incorporating the concept of the Compact State was used in conjunction with the ID technique, a simple numerical procedure to examine the subsidence/settlement of a sand layer supporting a bed of free draining or otherwise totally impervious overburden soil.

The results of the analysis indicate that the weight of the overburden reduces the magnitude of the ground subsidence provided that the overburden consists of free-draining material (or that a blanket of free-draining material exists between the sand and the surcharge).

If the surcharge is impervious (e.g. it consists of a layer of clay supported by the sand layer) then the settlement of the sand layer (and thus the eventual subsidence of the ground level) is independent of the magnitude of the surcharge (the thickness of the clay layer). In such a situation a film of water appears between the top of the sand layer and the clay layer shortly after the commencement of the ground shaking and thus the surcharge (clay layer) would be floating on a sea of water. Failure of footings, pavements, pipelines, etc. and the formation of sand volcanoes are various forms of instability caused by this phenomenon. Scott and Zuckerman (1967) had proposed the formation of the water interlayer film; the present paper quantifies its magnitude.

For any given pattern of ground shaking, the thickness of the water film appearing between the sand layer and the top clay layer (surcharge) is, of course, a function of the depth of the sand layer and its density. For the base excitation shown in Fig. 4, this dependence is shown in Fig. 12 for the sand layer void ratios ranging from 0.45 (very dense) to 0.85 (very loose). Thus in cases where deep foundations (extending to depth below the sand layer) can not be installed, either because of cost or the nature of the project, extensive damage can be prevented by provision of vertical drainage (by inclusion of stone columns for example) in conjunction with compaction of the sand layer (say by vibro-floatation).

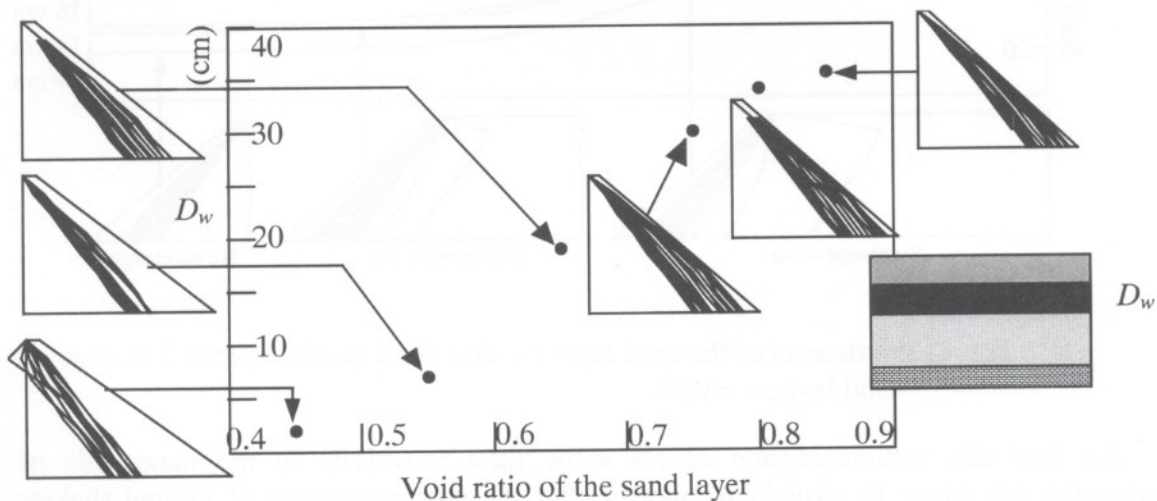


Fig. 12 Thickness of the layer of water between the sand layer and the surcharge, D_w vs. void ratio of a 3 m deep sand layer

Another point worthy of note is that in the case of impermeable top layer (surcharge) the interbedded sand layer liquefies (in the sense that the effective vertical stress approaches very small values) and hence would be unable to exert much resisting force to lateral movements. This conclusion would play a paramount role in the design of deep foundations such as piles or piers.

Two further comments conclude this paper. First, the distribution of pore water pressure versus depth/time curves related to the very dense sand layer (shown on the lowest left hand side corner of Fig. 12 indicate the development of a small negative p.w.p. for a short period during the shaking phase. This is expected as the layer is very dense and has a tendency to expand upon loading caused by the vibrations. Second, the thickness of the water layer, D_w , associated with the very high void ratio (extremely loose) sand layers appears to approach asymptotically a constant value of about 35 cm for the particular sand used in this study and

the loading program shown in Fig. 4. One explanation for this observation is that for such loose layers the sample approaches the liquefaction state very soon after the commencement of the ground shaking. This is evident from the figure on the upper right hand side corner of Fig. 12, which shows the distribution of the p.w.p. versus depth/time for such loose formations. After liquefaction waves can not be transmitted to elevations above the liquefied layer and no further densifications can take place above this elevation.

ACKNOWLEDGEMENT

The financial support from the Natural and Engineering Research Council (NSERC) of Canada in support of this work is gratefully acknowledged.

REFERENCES

- Dafalias, Y. F. and Popov, E. P. (1975). A model of non linearly hardening for cyclic loading. *Acta Mechanica*, 21: 173-192.
- Noorzad, A. (1998). Cyclic behavior of cohesionless granular media using the compact state concept. Ph.D. Thesis, Concordia University.
- Poorooshasb, H. B. and Noorzad, A. (1996). The compact state of the cohesionless granular media. *Scientia Iranica*, 3(1,2,3): 1-8.
- Poorooshasb, H. B., Alamgir, M. and Miura, N. (1996). Application of an integro-differential equation to the analysis of geotechnical problems. *Structural Engineering and Mechanics*, 4(3): 227-242.
- Roscoe, K. H. and Poorooshasb, H. B. (1963). A fundamental principle of similarity in model tests for earth pressure problems. *Proceedings of the 2nd Asian Regional Conference on Soil Mechanics and Foundation Engineering*, Tokyo, Japan.
- Scott, R. F., and Zuckerman, K. A. (1967). Sand blows and liquefaction. *The Great Alaskan Earthquake of 1964*, California Institute of Technology.